

# Comparison of Spherical and Cylindrical Mode Filtering Techniques for Reflection Suppression With mm-wave Antenna Measurements

Stuart F. Gregson

Department of Engineering Materials and Electrical Science  
National Physical Laboratory  
Teddington, UK  
stuart.gregson@npl.co.uk

Zhengrong Tian

Department of Engineering Materials and Electrical Science  
National Physical Laboratory  
Teddington, UK  
zhengrong.tian@npl.co.uk

**Abstract**—Reflections in antenna measurement ranges generally comprise the most significant component within the facility level uncertainty budget [1]. For more than a decade, a frequency domain measurement and mode filtering technique has been employed to significantly reduce range reflections within spherical near-field antenna test systems [2, 3]. More recently, this technique was adapted so that it could also be used with far-field antenna measurement systems [4, 5] and was firmly rooted in standard cylindrical near-field theory [6, 7, 8]. Although initially conceived as a means by which the frequency of operation of a given facility could be extended downwards to, *e.g.* UHF, where operation could otherwise be compromised by the limited performance of the absorber, these techniques have been used very successfully at frequencies much higher than this. However, this paper, for the first time, compares and contrasts the effectiveness of the approach at EHF frequencies and in particular at 190 GHz. This paper provides an introduction to the measurement techniques and offers a description of the mode filtering and post-processing algorithms before presenting preliminary results of actual range measurements and transformation using both spherical and cylindrical mode filtering of a mm-wave low gain horn antenna. These results illustrate the success of the techniques and examine the effect of various band-pass filter functions.

**Keywords**—*mm-wave, scattering suppression, spherical mode, cylindrical mode, filtering.*

## I. INTRODUCTION

When taking antenna measurements indoors, the effects of spurious scattered fields are largely managed by covering the interior of the chamber, and much of the measurement equipment, with RF absorbent material. This absorber is typically manufactured using open-cell Carbon impregnated foam which is bulky, costly, and has a performance that is tailored for use across a predetermined range of frequencies with inevitable degradation in performance outside of that band. Thus, any general purpose range is going to be compromised, to some extent, in the frequency limits. Thus, methods for extending the frequency band of operation of a given test system through mitigation of range multipath has received considerable attention in the open literature with significant time, effort and ingenuity being devoted to identifying and extracting range multipath contamination from measurements by means of: software or hardware time-gating, background pattern subtraction, Argand plane circular least squares function fitting and signal encoding based techniques being amongst the more widely encountered techniques. However, frequency domain

measurement and mode filtering based methods for scattering suppression and clutter rejection [9] have been known for three decades now, but it is only in the last dozen or so years that this technique has entered into the mainstream and become widely incorporated within all forms of antenna pattern measurement systems [10]. Initially, the technique was largely deployed to help extend the lower frequency of operation of spherical near-field antenna test systems where the degradation in the performance of the absorber would otherwise limit the use of the facility. Although the technique became more widely deployed at higher frequencies, comparatively few studies are available at mm-wave frequencies [11, 12]. Although at higher frequencies the spherical loss factor can, to some extent, be expected to provide a degree of immunity to the effects of range reflections, it is generally found that this does not entirely free the user from the requirement to manage this aspect of the measurement due to the corresponding reduction in physical size, which is a consequence of preserving the RF dynamic range, and the scattering resulting from the mechanical support and positioning equipment.

This paper presents the results of a recent test campaign that characterised a mm-wave, *circa* 20 dBi, horn antenna using spherical near-field (SNF) and direct far-field (FF) measurement methods. This is of particular interest as one of the more widely acknowledged limitations of taking direct far-field antenna pattern measurements is that range multipath effects can degrade the accuracy of the measurement to a greater extent than when using corresponding near-field (NF) methods. The reason for this is that there is no innate suppression of these scattering artefacts. This contrasts notably with NF testing methods which incorporate an integral transform that tends to suppress and mitigate some of these incoherent, uncorrelated reflected components. Thus, the effectiveness of the spherical and cylindrical far-field mode filtering based scattering suppression algorithms are examined, compared and contrasted herein with particular attention being paid to the effects of utilising a variety of different mode filtering functions. This paper concludes with a summary and presents an overview of the planned future work.

## II. OVERVIEW OF THE TECHNIQUES

It is well known that electromagnetic (EM) fields radiating into a linear, isotropic and homogeneous source or sink free region of free-space can be expanded onto a set of elementary orthogonal vector mode functions and that these

The authors gratefully acknowledge the funding support provided by the UK National Measurement System that enabled the work that this paper presents.

mode functions and their attendant complex amplitudes can be used to represent the electric and magnetic fields everywhere in space outside of the boundary surface over which those fields were matched, [6, 10, 13]. This principle is embodied, for example, within equations (1) and (2). In equations (1) and (2), the transverse magnetic (TM) and transverse electric (TE) vector wave, *i.e.* basis, functions are denoted by  $\underline{M}$  and  $\underline{N}$ , with the associated complex mode amplitudes being denoted by  $B^s$ . Conversely, the  $B^s$  mode coefficients can be obtained from the electric fields by inverting (1) and (2) using mode orthogonality [6, 10, 13].

$$\vec{E}(\vec{r}) = \sum_{n=1}^{\infty} \sum_{m=-n}^n \left[ B^{1mn} \vec{M}^{nm}(\vec{r}) + B^{2mn} \vec{N}^{nm}(\vec{r}) \right] \quad (1)$$

$$\vec{E}(\vec{r}) = \sum_{n=-\infty}^{\infty} \int_{-\infty}^{\infty} \left[ B_n^1(\gamma) \vec{M}_{n\gamma}^{(1)}(\vec{r}) + B_n^2(\gamma) \vec{N}_{n\gamma}^{(1)}(\vec{r}) \right] d\gamma \quad (2)$$

Here, the general form of these expansions is clearly very closely related, equation (1) expands the field onto a set of orthogonal spherical mode functions whereas equation (2) expands the fields onto an analogous set of orthogonal cylindrical mode functions [6, 10, 11].

Although a detailed development of the theoretical basis of the scattering suppression techniques is beyond the scope of this paper and can be found presented in the open literature [10], the following summary of the measurement and data post-processing may be of some utility to the reader.

1. Obtain the far electric field amplitude and phase pattern function with the AUT when offset, *i.e.* displaced, from the origin.
2. Mathematically translate the AUT back to the origin of the measurement coordinate system with, for example, the application of a differential phase change.
3. Solve for the translated mode coefficients of the AUT when conceptually located at the origin of the measurement coordinate system.
4. Apply a mode filtering function to suppress unwanted higher order mode coefficients where the properties of the filter function are determined from the physical size of the AUT and the frequency.
5. Compute the complete far electric field pattern from the filtered mode coefficients to obtain the filtered antenna pattern function.

Close inspection of the various implementations of the scattering suppression technique, *e.g.* [2, 3, 4, 5, 10], reveal that each is predicated upon the use of a modal expansion, as embodied within equations (1) and (2), an isometric translation of origins, and a modal filtering, clutter rejection, operation. Thus, it is evident that the underlying principle is not a “peculiarity” of any one specific modal expansion or sampling scheme, *etc.* but rather is a far more ubiquitous principle that enables a distinction to be drawn between those fields being emitted from an antenna under test (AUT) and the fields arising from range reflection that is entirely independent of the details of the exact mathematical treatment being employed. Although the spherical processing is based around (1), the far-field implementation is actually predicated on (2), the asymptotic infinite radius far-field form of (2) exhibits the attractive attribute that the processing can be deployed, without further approximation, using only a singularly polarised, great circle, one-dimensional, far-field antenna pattern cut comprising amplitude and phase data [4, 5, 10]. This is very significant,

as one of the most compelling attributes of far-field testing is its ability to provide a single antenna pattern cut, thereby minimizing the required measurement time and complexity. Any NF technique is predicated upon acquiring the majority of the radiated field over a two dimensional acquisition interval which inevitably requires lengthier measurement times.

### III. SPHERICAL NEAR-FIELD AND FAR-FIELD SCATTERING SUPPRESSION RESULTS

As was set out above, step 4 requires the reconstructed translated mode coefficients be filtered to extract modes associated with the scattered fields. A number of windowing functions are in common use today and as part of this study their impact on the processed far-field pattern was assessed. The three windowing functions were:

- 1) Brick-wall (rectangular) filter function,

$$f_n = \begin{cases} 1 & \text{when } |n| \leq n_{\max} \\ 0 & \text{elsewhere} \end{cases} \quad (3)$$

- 2) Conventional “MARS” filter function [14],

$$f_n = \begin{cases} 1 & \text{when } |n| \leq n_{\max} \\ 0.5^{|n|-n_{\max}} & \text{elsewhere} \end{cases} \quad (4)$$

- 3) Tapered cosine squared filter function which has the benefit of matching the windowed function and its first derivative to zero at the boundaries,

$$f_n = \begin{cases} 1 & \text{when } |n| \leq n_{\max} \\ \frac{1}{4} \left[ 1 + \cos \left( \frac{\pi (|n| - n_{\max})}{n_{\text{Highest}} - n_{\max}} \right) \right]^2 & \text{elsewhere} \end{cases} \quad (5)$$

Many other filter functions exist however these particular functions were chosen as they are some of the more commonly encountered variants. These functions can be seen illustrated in Fig 1. below together with the cylindrical mode coefficients (CMC) that were obtained from the 190 GHz measurement of the horn AUT. The effect that they have on the filtered mode spectrum is illustrated in Fig. 2.

The question of which modes should be retained and which should be discarded by the filtering process is crucial if reliable far-field patterns are to be produced. This question can be addressed with the use of the sampling theorem [6, 10, 13].

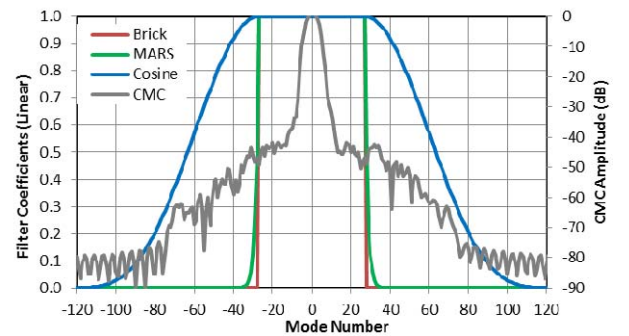


Fig. 1. Illustration of the three windowing functions together with the CMCs of the mm-wave horn antenna.

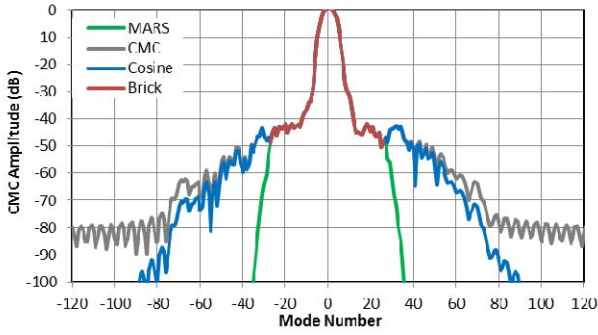


Fig. 2. Comparison of CMCs with and without filtering.

When translated back to the origin of the measurement coordinate system, it is assumed that the antenna under test (AUT) can then be enclosed within a minimum sphere (or cylinder) of radius  $\rho_0$ . Here,  $\rho_0$  denotes the Maximum Radial Extent (MRE) which is measured from the origin of the measurement coordinate system and is large enough to enclose the majority of the current sources. That is to say, modes of order  $n_{max} > k_0\rho_0$  are needed to represent the most complex components of the field structure thus typically  $n_{max}$  is chosen so that [6, 10, 13],

$$n_{max} = \text{ceil}(k_0\rho_0) + n_1 \quad (6)$$

Here,  $\text{ceil}$  is used to denote a function that rounds to the nearest integer towards positive infinity, and  $n_1$  is a positive integer that depends upon the accuracy required. The following section presents results of the range measurements and the various scattering suppression algorithms, highlighting the effects of utilising the various filter functions defined above.

#### IV. COMPARISON OF CYLINDRICAL AND SPHERICAL MODE FILTERING USING A VARIETY OF WINDOWING FUNCTIONS

The cylindrical and spherical mode based scattering suppression techniques were examined using measurements taken of a mm-wave circular horn antenna which was acquired at 190 GHz. The AUT was mounted on a conventional  $\phi$  over  $\theta$  polar-spherical positioner system [10] with the aperture of the AUT offset from the vertical  $\theta$ -axis by 10 mm. This is a little over 6 wavelengths and is a distance that is a little larger than the diameter of the aperture of the AUT which has been found to be, in many cases, the optimum offset, *cf.* [10]. The test range used to acquire this data was housed within a temperature controlled ( $23 \pm 1^\circ\text{C}$ ) 15m long by 7.5m wide by 7.5m high fully anechoic chamber. Conventional spherical data was acquired and subsequently transformed to the far-field using a standard spherical near-field to far-field transform. This data was then processed using the spherical and cylindrical mode based scattering suppression processing described in the preceding section.

Fig. 3 below presents, respectively, azimuth (left) and elevation (right) great circle pattern cuts of the copolar pattern of the mm-wave horn antenna when measured at 190 GHz. Here, three traces are shown, the back trace shows the far-field pattern of the horn, the red trace shows the far-field pattern when the SMCs have been filtered using the brick-wall filter function, the green trace shows the equivalent pattern when the modes have been filtered using the conventional ‘‘MARS’’ filter function [14]. Here, it is

evident that in each case the mode filtering has effectively suppressed the high angular frequency ripple that is evident on the wide-out antenna pattern that is recognised as being an artefact of scattering. However, the tapered ‘‘MARS’’ filtering function has suppressed the undesirable ringing that is evident on the pattern when a brick-wall filter function is used. Here, the processing was based upon using the SMCs which necessitated the use of the entire 2D FF pattern.

Fig. 4 below presents similar results to those shown in Fig. 3. However here, four traces are shown. The back trace shows the far-field pattern of the horn, the red trace shows the far-field pattern when the CMCs have been filtered using the brick-wall filter function, the green trace shows the equivalent pattern when the modes have been filtered using the conventional ‘‘MARS’’ filter function, and the blue trace denotes the use of the cosine squared filter function. From inspection of these plots it is again evident that in each case the mode filtering has effectively suppressed the high angular frequency ripple that is evident on the wide-out antenna pattern that is recognised as being an artefact of scattering. Here, the processing was based upon using the CMCs which necessitated the use of only a single 1D FF pattern cut, which was successively chosen to be the horizontal, *i.e.* azimuth, and vertical, *i.e.* elevation, pattern cuts.

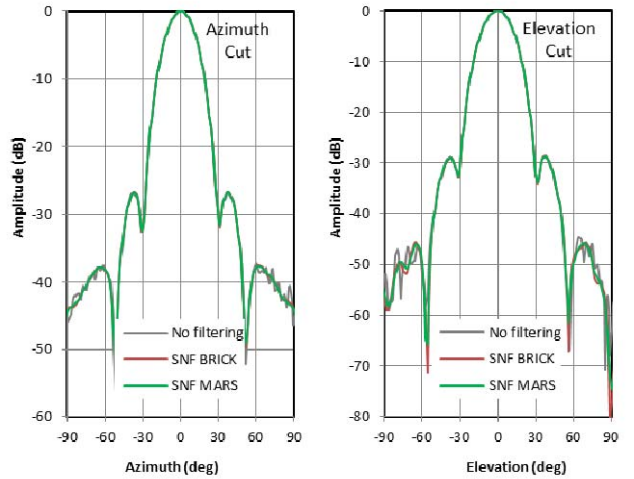


Fig. 3. Comparison of azimuth (left) and elevation (right) great circle far-field pattern cuts with and without spherical mode filtering.

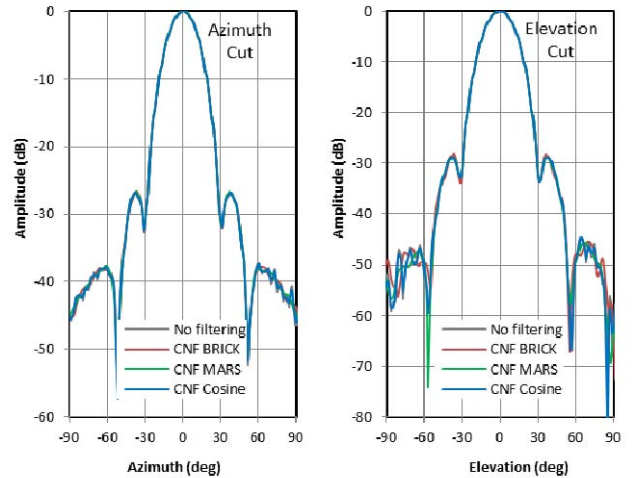


Fig. 4. Comparison of azimuth (left) and elevation (right) great circle far-field pattern cuts with and without cylindrical mode filtering.

By inspection of Fig 3. and 4. it can be observed that for both spherical and cylindrical transformation, the “MARS” filter offers best filtering capability in terms of suppression of the higher order modes. It is however worth noting that the degree of rejection of scattering is better when using the spherical processing. The primary reason for this is that the CMC based processing operates on a single 1D pattern cut whereas the SMC based processing utilises the entire 2D pattern function. This means that the SMC based processing is able to suppress scattered signals in two-dimensions whereas the 1D CMC based processing is not able to effectively suppress scattering terms that are propagating in a plane that is orthogonal to that which the pattern cut resides.

A closer comparison of the cylindrical and spherical mode processing results is presented below in Fig. 5 where the azimuth (left) and elevation (right) far-field pattern cuts are presented. Here, the black trace shows the far-field pattern of the horn, the red trace shows the far-field pattern when the CMCs have been filtered, the green trace shows the equivalent pattern when the SMCs have been filtered and the blue trace denotes the dB difference level [10] between the respective mode filtered results. The closer the degree of agreement attained between the respective results, then the larger the negative dB value becomes. From inspection of Fig 5. it can be seen that the stray signal level (SSL) is *circa* 20 dB below the pattern level in the wide-out side-lobe region where the pattern itself is approximately 40 dB below the level of the main beam peak. This is a very encouraging result especially when considering the frequency that these results were taken at.

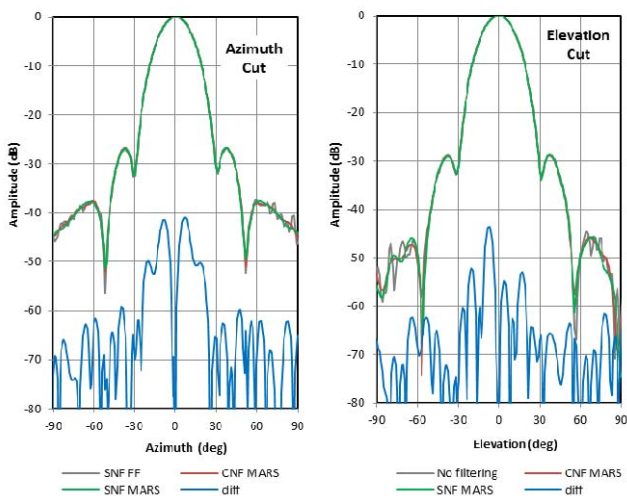


Fig. 5. Comparison of pattern cuts through spherical and cylindrical transformation using MARS filter and showing difference level.

## V. SUMMARY AND CONCLUSIONS

For the first time, this paper recounts the successful use of spherical and cylindrical based mode-filtering techniques for the suppression of range reflections on antenna pattern measurements taken at 190 GHz. Additionally, and also for the first time, this paper presents results of the successful comparison of mode filtering results that were based upon techniques using one-dimensional great circle far-field pattern cut and CMC based processing by comparison with results obtained from two-dimensional pattern data and a SMC based processing technique. It is important to recognise that the CMC based approach has a very

significant practical value in terms of measurement efficiency for cases where only the pattern cuts, including any inter-cardinal pattern cuts, are of interest. Within this study, a number of different mode filtering functions were compared and contrasted. Of the functions examined, the classical “MARS” [14] windowing function provided the best compromise between immunity from scattering and minimum ringing on the resulting far-field antenna patterns.

As no absolute truth-model is currently available, the planned future work is to include recreating the measurement configuration within a three-dimensional full-wave computation electromagnetic (CEM) solver so that the scattering suppression technique can be more closely, quantitatively examined, compared and contrasted. In this way, it is anticipated that the success of a wider variety of, perhaps less conventional, windowing functions may be explored.

## REFERENCES

- [1] A.C. Newell, “Error Analysis Techniques for Planar Near-field Measurements”, IEEE Transactions on Antennas and Propagation, vol. AP-36, pp. 754-768, June 1988.
- [2] G.E. Hindman, A.C. Newell, “Reflection Suppression in a large spherical near-field range”, AMTA 27th Annual Meeting & Symposium, Newport, RI, October. 2005.
- [3] G.E. Hindman, A.C. Newell, “Reflection Suppression To Improve Anechoic Chamber Performance”, AMTA Europe 2006, Munch, Germany, March 2006.
- [4] S.F. Gregson, B.M. Williams, G.F. Masters, A.C. Newell, G.E. Hindman, “Application of Mathematical Absorber Reflection Suppression To Direct Far-Field Antenna Range Measurements”, AMTA, Denver, October 2011.
- [5] S.F. Gregson, J. Dupuy, C.G. Parini, A.C. Newell, G.E. Hindman, “Application of Mathematical Absorber Reflection Suppression to Far-Field Antenna Testing”, LAPC, Loughborough, November, 2011. FF MARS AMTA
- [6] A.D. Yaghjian, “Near-Field Antenna Measurements On a Cylindrical Surface: A Source Scattering Matrix Formulation”, NBS Technical Note 696, 1977.
- [7] S.F. Gregson, A.C. Newell, G.E. Hindman, “Reflection Suppression In Cylindrical Near-Field Antenna Measurement Systems – Cylindrical MARS”, AMTA 31st Annual Meeting & Symposium, Salt Lake City, UT, November 2009.
- [8] S.F. Gregson, A.C. Newell, G.E. Hindman, “Reflection Suppression In Cylindrical Near-Field Measurements of Electrically Small Antennas”, Loughborough Antennas & Propagation Conference, November, 2009.
- [9] O.M. Bucci, G. D’Elia, M.D. Migliore, “A General and Effective Clutter Filtering Strategy in Near-Field Antenna Measurements”, IEEE Proc.-Microwave Antennas and Propagation, Vol. 151, No. 3, June 2004.
- [10] C.G. Parini, S.F. Gregson, J. McCormick, D. Janse van Rensburg “Theory and Practice of Modern Antenna Range Measurements”, IET Press, 2014, ISBN 978-1-84919-560-7.
- [11] F. Ferrero, Y. Benoit, L. Brochier, J. Lanteri, J-Y Dauvignac, C. Migliaccio, S.F. Gregson, “Spherical Scanning Measurement Challenge for Future Millimeter Wave Applications”, AMTA Symposium, Long Beach, California, USA, October, 2015.
- [12] D. Janse van Rensburg, “Factors limiting the upper frequency of mm-wave spherical near-field test systems”, EUCAP 2015, Lisbon, Portugal, April, 2015.
- [13] J.E. Hansen (ed.), “Spherical Near-Field Antenna Measurements”, IET, UK, Peter Peregrinus Ltd., 1988.
- [14] S.F. Gregson, A.C. Newell, P.N. Betjes, C.G. Parini, “Verification of Spherical Mathematical Absorber Reflection Suppression in a Combination Spherical Near-Field and Compact Antenna Test Range”, AMTA Symposium, Atlanta Georgia, October, 2017.